# 11
Compartment Fires

11.1 Introduction

The subject of compartment fires embraces the full essence of fire growth. The 'compartment' here can represent any confined space that controls the ultimate air supply and thermal environment of the fire. These factors control the spread and growth of the fire, its maximum burning rate and its duration. Although simple room configurations will be the limit of this chapter, extensions can be made to other applications, such as tunnel, mine and underground fires. Spread between compartments will not be addressed, but are within the scope of the state-of-the-art. A more extensive treatment of enclosure fires can be found in the book by Karlsson and Quintiere [1]. Here the emphasis will be on concepts, the interaction of phenomena through the conservation equations, and useful empirical formulas and correlations. Both thermal and oxygen-limiting feedback processes can affect fire in a compartment. In the course of fire safety design or fire investigation in buildings, all of these effects, along with fire growth characteristics of the fuel, must be understood. The ability to express the relevant physics in approximate mathematics is essential to be able to focus on the key elements in a particular situation. In fire investigation analyses, this process is useful to develop, first, a qualitative description and then an estimated time-line of events. In design analyses, the behavior of fire growth determines life safety issues, and the temperature and duration of the fire controls the structural fire protection needs. While such design analysis is not addressed in current prescriptive regulations, performance codes are evolving in this direction. The SFPE *Guide to Fire Exposures* is an example [2]. Our knowledge is still weak, and there are many features of building fire that need to be studied. This chapter will present the basic physics. The literature will be cited for illustration and information, but by no means will it constitute a complete review. However, the work of Thomas offers much, e.g. theories (a) on wood crib fires [3], (b) on flashover and instabilities [4,5], and (c) on pool fires in compartments [6].
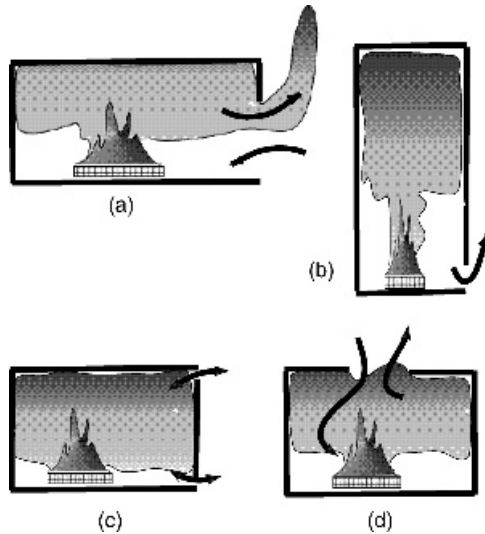
**Figure 11.1**   Compartment fire scenarios

11.1.1   *Scope*

The scope of this chapter will focus on typical building compartment fires representative of living or working spaces in which the room height is nominally about 3 m. This scenario, along with others, is depicted in Figure 11.1, and is labeled (a). The other configurations shown there can also be important, but will not necessarily be addressed here. They include:

(b) tall, large spaces where the contained oxygen reservoir is important;

(c) leaky compartments where extinction and oscillatory combustion have been observed (Tewarson [7], Kim, Ohtami and Uehara [8], Takeda and Akita [9]);

(d) compartments in which the only vent is at the ceiling, e.g. ships, basements, etc.

Scenario (a) will be examined over the full range of fire behavior beginning with spread and growth through 'flashover' to its 'fully developed' state. Here, flashover is defined as a transition, usually rapid, in which the fire distinctly grows bigger in the compartment. The fully developed state is where all of the fuel available is involved to its maximum extent according to oxygen or fuel limitations.

11.1.2   *Phases of fires in enclosures*

Fire in enclosures may be characterized in three phases. The first phase is fire development as a fire grows in size from a small incipient fire. If no action is taken to suppress the fire, it will eventually grow to a maximum size that is controlled by the
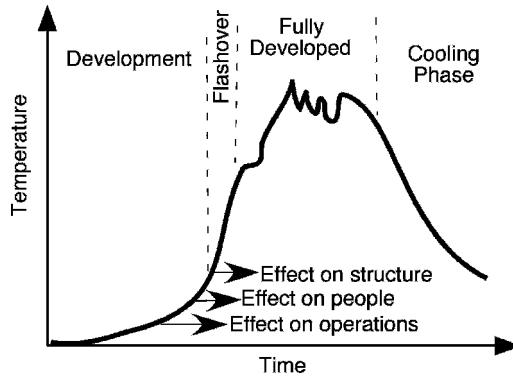
Figure 11.2 Phases of fire development

amount of fuel present (fuel controlled) or the amount of air available through ventilation openings (ventilation limited). As all of the fuel is consumed, the fire will decrease in size (decay). These stages of fire development can be seen in Figure 11.2.

The fully developed fire is affected by (a) the size and shape of the enclosure, (b) the amount, distribution and type of fuel in the enclosure, (c) the amount, distribution and form of ventilation of the enclosure and (d) the form and type of construction materials comprising the roof (or ceiling), walls and floor of the enclosure. The significance of each phase of an enclosure fire depends on the fire safety system component under consideration. For components such as detectors or sprinklers, the fire development phase will have a great influence on the time at which they activate. The fully developed fire and its decay phase are significant for the integrity of the structural elements.

Flashover is a term demanding more attention. It is a phenomenon that is usually obvious to the observer of fire growth. However, it has a beginning and an end; the former is the connotation for flashover onset time given herein. In general, flashover is the transition between the developing fire that is still relatively benign and the fully developed fire. It usually also marks the difference between the fuel-controlled or well-ventilated fire and the ventilation-limited fire. The equivalence ratio is less than 1 for the former and greater than 1 for the latter, as it is fuel-rich. Flashover can be initiated by several mechanisms, while this fire eruption to the casual observer would appear to be the same. The observer would see that the fire would 'suddenly' change in its growth and progress to involving all of the fuel in the compartment. If the compartment does not get sufficient stoichiometric air, the fire can produce large flames outside the compartment. A ventilation-limited fire can have burning mostly at the vents, and significant toxicity issues arise due to the incomplete combustion process. Mechanisms of flashover can include the following:

1. *Remote ignition.* This is the sudden ignition by autoignition or piloted ignition, due to flaming brands, as a result of radiant heating. The radiant heating is principally from the compartment ceiling and hot upper gases due to their large extent. The threshold for the piloted ignition of many common materials is about 20 kW/m^2. This value of flux, measured at the floor, is commonly taken as an operational criterion for flashover. It also corresponds to gas temperatures of 500–600 °C.

2. *Rapid flame spread.* As we know, radiant preheating of a material can cause its surface temperature to approach its piloted ignition temperature. This causes a singularity in simple flame spread theory that physically means that a premixed mixture at its lower flammability limit occurs ahead of the surface flame. Hence, a rapid spread results in the order of 1 m/s.

3. *Burning instability.* Even without spread away from a burning item, a sudden fire eruption can be recognized under the right conditions. Here, the thermal feedback between the burning object and the heated compartment can cause a 'jump' from an initial stable state of burning at the unheated, ambient conditions, to a new stable state after the heating of the compartment and the burning of the fuel come to equilibrium.

4. *Oxygen supply.* This mechanism might promote back-draft. It involves a fire burning in a very ventilation-limited state. The sudden breakage of a window or the opening of a door will allow fresh oxygen to enter along the floor. As this mixes with the fuel-rich hot gases, a sudden increase in combustion occurs. This can occur so rapidly that a significant pressure increase will occur that can cause walls and other windows to fail. It is not unlike a premixed gas 'explosion'.

5. *Boilover.* This is a phenomenon that occurs when water is sprayed on to a less dense burning liquid with a boiling temperature higher than that of water. Water droplets plunging through the surface can become 'instant' vapor, with a terrific expansion that causes spraying out of the liquid fuel. The added increase of area of the liquid fuel spray can create a tremendous increase in the fire. Even if this does not happen at the surface, the collection of the heavier water at the bottom of a fuel tank can suddenly boil as the liquid fuel recedes to the bottom. Hence, the term 'boilover'.

11.2   Fluid Dynamics

The study of fire in a compartment primarily involves three elements: (a) fluid dynamics, (b) heat transfer and (c) combustion. All can theoretically be resolved in finite difference solutions of the fundamental conservation equations, but issues of turbulence, reaction chemistry and sufficient grid elements preclude perfect solutions. However, flow features of compartment fires allow for approximate portrayals of these three elements through global approaches for prediction. The ability to visualize the dynamics of compartment fires in global terms of discrete, but coupled, phenomena follow from the flow features.

11.2.1   General flow pattern

The stratified nature of the flow field due to thermally induced buoyancy is responsible for most of the compartment flow field. Figure 11.3 is a sketch of a typical flow pattern in a compartment.

Strong buoyancy dominates the flow of the fire. Turbulence and pressure cause the ambient to mix (entrainment) into the fire plume. Momentum and thermal buoyancy
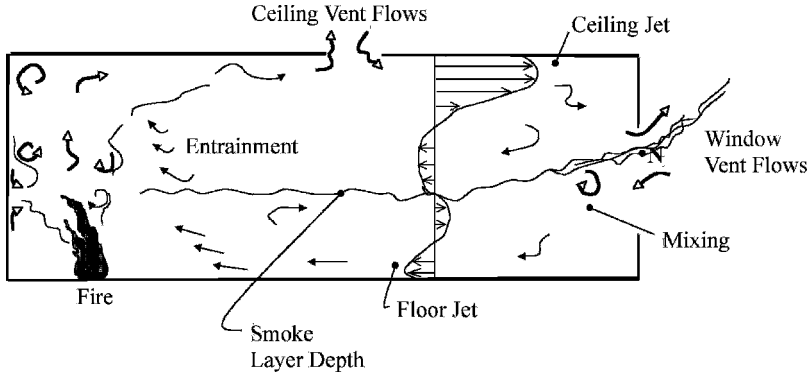
**Figure 11.3**   Flow pattern in a compartment fire

causes a relatively thin ceiling jet to scrub the ceiling. Its thickness is roughly one-tenth of the room height. A counterpart cold floor jet also occurs. In between these jets, recirculating flows form in the bulk of the volume, giving rise to a four-layer flow pattern. At the mid-point of this four-layer system is a fairly sharp boundary (layer interface) due to thermal stratification between the relatively hot upper layer and cooler lower layer. Many of these flow attributes are displayed in photographs taken by Rinkinen [10] for 'corridor' flows, made visible by white smoke streaks Figure 11.4. Figure 11.5 shows the sharp thermal stratification of the two layers in terms of the gas or wall temperatures [11].

11.2.2   *Vent flows*

The flow of fluids through openings in partitions due to density differences can be described in many cases as an orifice-like flow. Orifice flows can be modeled as inviscid Bernoulli flow with an experimental correction in terms of a flow coefficient, C, which generally depends on the contraction ratio and the Reynolds number. Emmons [12] describes the general theory of such flows. For flows through horizontal partitions, at near zero pressure changes, the flow is unstable and oscillating bidirectional flow will result. In this configuration, there is a flooding pressure above which unidirectional Bernoulli flow will occur. Epstein [13] has developed correlations for flows through horizontal partitions. Steckler, Quintiere and Rinkinen [14] were the first to measure successfully the velocity and flow field through vertical partitions for fire conditions. An example of their measured flow field is shown in Figure 11.6 for a typical module room fire.

The pressure difference promoting vertical vent flows are solely due to temperature stratification, and conform to a hydrostatic approximation. In other words, the momentum equation in the vertical direction is essentially, due to the low flows:

$$\frac{\partial p}{\partial z} = -\rho g \tag{11.1}$$
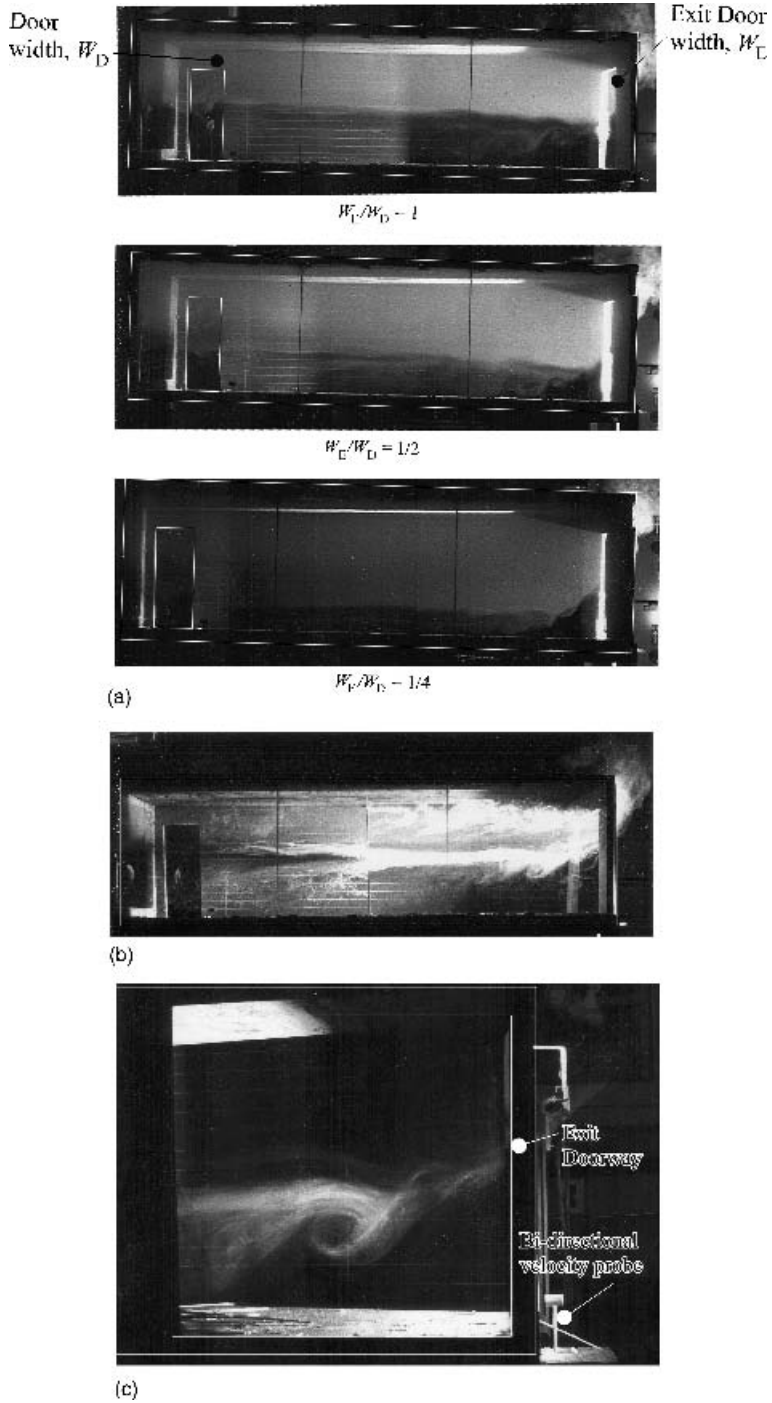
Figure 11.4   (a) Smoke layers in a model corridor as a function of the exit door width (b) Smoke streaklines showing four directional flows (c) Smoke streaklines showing mixing of the inlet flow from the right at the vent with the corridor upper layer [10]
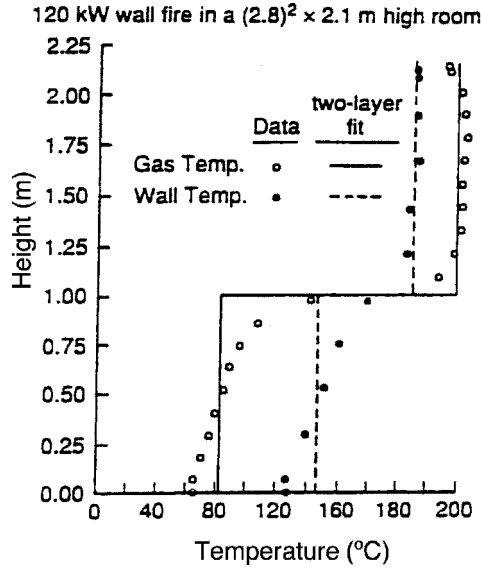
Figure 11.5   Thermal layers [11]

From Figure 11.3, under free convection, there will be a height in the vent at which the flow is zero, N; this is called the neutral plane. The pressure difference across the vent from inside (i) to outside (o) can be expressed above the neutral plane as

$$p_{\mathrm{i}} - p_{\mathrm{o}} = \int_0^z (\rho_{\mathrm{o}} - \rho_{\mathrm{i}})g \ \mathrm{d}z \tag{11.2}$$
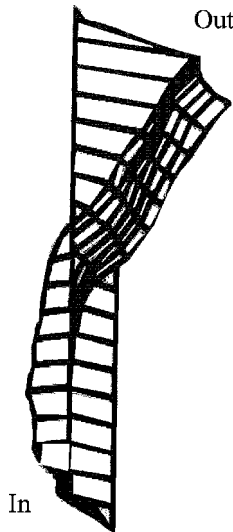

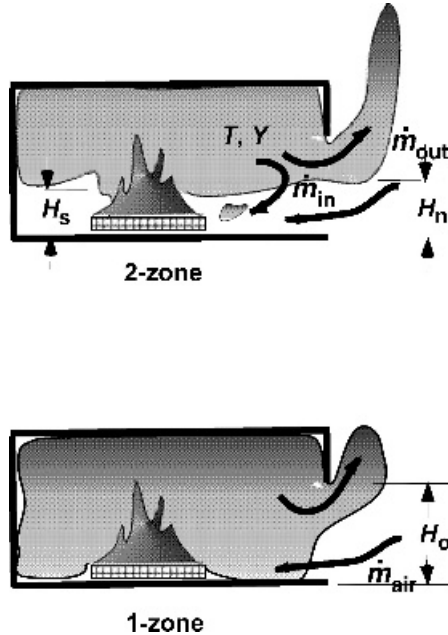**Figure 11.6**   Measured flow field in the doorway of a room fire [14]

Figure 11.7   Zone modeling concepts

Such pressure differences are of the order of 10 Pa for $z \sim 1$ m and therefore these flows are essentially at constant pressure (1 atm $\approx 10^5$ Pa). The approach to computing fire flows through vertical partitions is to: (a) compute velocity from Bernoulli's equation using Equation (11.2), (b) substitute temperatures for density using the perfect gas law and, finally, (c) integrate to compute the mass flow rate. This ideal flow rate is then adjusted by a flow coefficient generally found to be about 0.7 [12,14]. Several example flow solutions for special cases will be listed here. Their derivations can be found in the paper by Rockett [15]. The two special cases consider a two-zone model in which there is a hot upper and lower cool homogeneous layer as shown in Figure 11.7(a); this characterizes a developing fire. Figure 11.7(b) characterizes a large fully developed fire as a single homogeneous zone.

The two-zone model gives the result in terms of the neutral plane height (H_n) and the layer height (H_s) for a doorway vent of area A_o and height H_o. The ambient to room temperature ratio is designated as $\theta \equiv T_o/T$:

$$\dot{m}_{out} = \tfrac{2}{3}\sqrt{2g}C\rho_o A_o \sqrt{H_o}[(\theta)(1-(\theta))]^{1/2}\left[\tfrac{1-H_n}{H_o}\right]^{3/2} \tag{11.3}$$

$$\dot{m}_{in} = \tfrac{2}{3}\sqrt{2g}C\rho_o A_o \sqrt{H_o}[1-(\theta)]^{1/2}\left(\tfrac{H_n}{H_o}-\tfrac{H_s}{H_o}\right)^{1/2}\left(\tfrac{H_n}{H_o}+\tfrac{H_s}{2H_o}\right) \tag{11.4}$$

The inflow is generally the ambient air and the outflow is composed of combustion products and excess air or fuel.

For a one-zone model under steady fire conditions, the rate mass of air inflow can be further computed in terms of the ratio of fuel to airflow rate supplied (μ) as

$$\dot{m}_{\text{air}} = \frac{\frac{2}{3}\rho_{\text{o}}CA_{\text{o}}\sqrt{H_{\text{o}}}\sqrt{g}\sqrt{2(1-\theta)}}{\left[1 + [(1+\mu)^2/\theta]^{1/3}\right]^{3/2}} \tag{11.5}$$

It is interesting to contrast Equation (11.5) with the air flow rate at a horizontal vent under bidirectional, unstable flow from Epstein [13]:

$$\dot{m}_{\text{air}} = \frac{0.068\rho_{\infty}A_{\text{o}}^{5/4}\sqrt{g}\sqrt{2(1-\theta)}}{(1+\theta)^{1/2}} \tag{11.6}$$

This horizontal vent flow is nearly one-tenth of that for the same size of vertical vent. Thus, a horizontal vent with such unstable flow, as in a basement or ship fire, is relatively inefficient in supplying air to the fire.

A useful limiting approximation for the air flow rate into a vertical vent gives the maximum flow as

$$\dot{m}_{\text{air}} = k_{\text{o}}A_{\text{o}}\sqrt{H_{\text{o}}}, \quad \text{where } k_{\text{o}} = 0.5 \text{ kg/s m}^{5/2} \tag{11.7}$$

This holds for $\theta < \frac{2}{3}$, and H_{s} small. In general, it is expected that $H_{\text{n}}/H_{\text{o}}$ ranges from 0.3 to 0.7 and $H_{\text{s}}/H_{\text{o}}$ from 0 to 0.6 for doorways [15].

11.3 Heat Transfer

The heat transfer into the boundary surface of a compartment occurs by convection and radiation from the enclosure, and then conduction through the walls. For illustration, a solid boundary element will be represented as a uniform material having thickness, δ, thermal conductivity, k, specific heat, c, and density, ρ. Its back surface will be considered at a fixed temperature, T_{o}.

The heat transfer path through the surface area, A, can be represented as an equivalent electric circuit as shown in Figure 11.8. The thermal resistances, or their inverses, the conductances, can be computed using standard heat transfer methods. Some will be illustrated here.
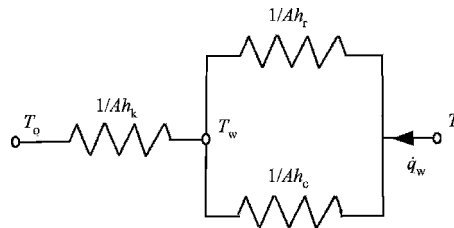
Figure 11.8 Wall heat transfer

11.3.1   Convection

Convections to objects in a fire environment usually occur under natural convection conditions. Turbulent natural convection is independent of scale and might be estimated from

$$Nu = \frac{h_c H}{K} = 0.13 \left[\left(\frac{g(T - T_o)H^3}{T\nu^2} \right) Pr \right]^{1/3} \tag{11.8a}$$

where ν is the kinematic viscosity and Pr is the Prandt number. It gives h_c of about 10 W/m^2 K. Under higher flow conditions, it is possible that h_c might be as high as 40 W/m^2 K. This has been shown in measurements by Tanaka and Yamada [16] as the floor-to-ceiling coefficients vary from about 5 to 40 W/m^2 K. They found that an empirical correlation for the average compartment convection coefficient is

$$\frac{\bar{h}_c}{\rho_\infty c_p \sqrt{gH}} = \begin{cases} 2.0 \times 10^{-3}, & Q_H^* \leq 4 \times 10^{-3} \\ 0.08 Q_H^{*2/3}, & Q_H^* > 4 \times 10^{-3} \end{cases} \tag{11.8b}$$

Q_H^* is based on height, H (see Equation (10.41)).

11.3.2   Conduction

Only a finite difference numerical solution can give exact results for conduction. However, often the following approximation can serve as a suitable estimation. For the unsteady case, assuming a semi-infinite solid under a constant heat flux, the exact solution for the rate of heat conduction is

$$\dot{q}_w = A \sqrt{\frac{\pi}{4} \frac{k\rho c}{t}} (T_w - T_o) \tag{11.9}$$

or, following Figure 11.8,

$$h_k = \sqrt{\frac{\pi}{4} \frac{k\rho c}{t}} \tag{11.10}$$

For steady conduction, the exact result is

$$h_k = \frac{k}{\delta} \tag{11.11}$$

The steady state result would be considered to hold for time,

$$t > \frac{\delta^2}{4[k/\rho c]} \tag{11.12}$$

approximately, from Equation (7.35).

Table 11.1 Approximate thermal properties for typical building material

	Concrete/brick	Gypsum	Mineral wool
k (W/m K)	1	0.5	0.05
$k\rho c$ (W^2 s/m^4 K^2)	10^6	10^5	10^3
$k/\rho c$ (m^2/s)	5×10^{-7}	4×10^{-7}	5×10^{-7}

Table 11.1 gives some typical properties. An illustration for a wall six inches thick, or $\delta \approx 0.15$ m, gives, for most common building materials,

$$t = \frac{\delta^2}{4[k/\rho c]} = 3.1 \text{ hours}$$

from Equation (11.12) for the thermal penetration time. Hence, most boundaries might be approximated as thermally thick since compartment fires would typically have a duration of less than 3 hours.

Since the thermally thick case will predominate under most fire and construction conditions, the conductance can be estimated from Equation (11.10). Values for the materials characteristic of Table 11.1 are given in Table 11.2. As time progresses, the conduction heat loss decreases.

11.3.3   Radiation

Radiation heat transfer is very complex and depends on the temperature and soot distribution for fundamental computations. Usually, these phenomena are beyond the state-of-the-art for accurate fire computations. However, rough approximations can be made for homogeneous gray gas approximations for the flame and smoke regions. Following the methods in common texts (e.g. Karlsson and Quintiere [1]) formulas can be derived. For example, consider a small object receiving radiation in an enclosure with a homogeneous gray gas with gray uniform walls, as portrayed in Figure 11.9. It can be shown that the net radiation heat transfer flux received is given as
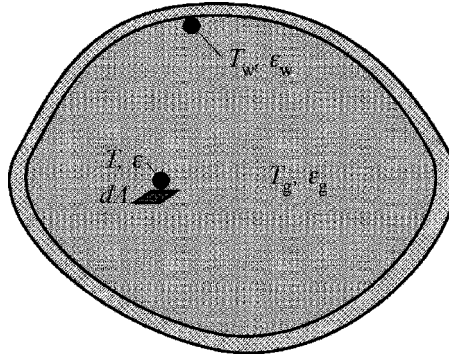
$$\dot{q}_r^{''} = \epsilon \left[\sigma(T_g^4 - T^4) - \epsilon_{wg}\sigma(T_g^4 - T_w^4) \right] \tag{11.13}$$

and

$$\epsilon_{wg} = \frac{(1 - \epsilon_g)\epsilon_w}{\epsilon_w + (1 - \epsilon_w)\epsilon_g}$$

Table 11.2 Typical wall conductance values

t(min)	h_k(W/m^{2}K)
10	0.8–26
30	0.3–10
120	0.2–5

Figure 11.9   Radiation of a small object in an enclosure

where

ϵ = emissivity of the target

ϵ_{w} = emissivity of the wall

ϵ_{g} = emissivity of the gas

T = target temperature

T_{w} = wall temperature

T_{g} = gas temperature

and

σ = Stefan–Boltzmann constant = 5.67×10^{-11} kW/m^{2}K^4

If the object is the wall itself, then Equation (11.13) simplifies to the rate of radiation received by the wall as

$$\dot{q}_{r} = \frac{A\sigma(T^4 - T_{w}^4)}{1/\epsilon_{g} + 1/\epsilon_{w} - 1} \tag{11.14}$$

Since the boundary surface will become soot-covered as the fire moves to a fully developed fire, it might be appropriate to set $\epsilon_{w} = 1$.

The gas emissivity can be approximated as

$$\epsilon_{g} = 1 - e^{-\kappa H} \tag{11.15}$$

where H represents the mean beam length for the enclosure that could be approximated as its height. The absorption coefficient of the smoke or flames, κ, could range from about 0.1 to 1 m^{-1}. For the smoke conditions in fully developed fires, $\kappa = 1$ m^{-1} is a reasonable estimate, and hence ϵ_{g} could range from about 0.5 for a small-scale laboratory enclosure to nearly 1 for building fires.

Under fully developed conditions, the radiative conductance can be expressed as

$$h_r = \epsilon_g \sigma (T^2 + T_w^2)(T + T_w) \tag{11.16}$$

It can be estimated, for $\epsilon_g = 1$ and $T = T_w$, that $h_r = 104 - 725$ W/m^2 K for $T = 500 - 1200\,°$C.

11.3.4 Overall wall heat transfer

From the circuit in Figure 11.7, the equivalent conductance, h, allows the total heat flow rate to be represented as

$$\dot{q}_w = hA(T - T_o) \tag{11.17a}$$

where

$$\frac{1}{h} = \frac{1}{h_c + h_r} + \frac{1}{h_k} \tag{11.17b}$$

For a fully developed fire, conduction commonly overshadows convection and radiation; therefore, a limiting approximation is that $h \approx h_k$, which implies $T_w \approx T$. This result applies to structural and boundary elements that are insulated, or even to concrete structural elements. This boundary condition is 'conservative' in that it gives the maximum possible compartment temperature.

11.3.5 Radiation loss from the vent

From Karlsson and Quintiere [1], it can be shown that for an enclosure with blackbody surfaces ($\epsilon_w = 1$), the radiation heat transfer rate out of the vent of area A_o is

$$\dot{q}_r = A_o \epsilon_g \sigma (T_g^4 - T_o^4) + A_o(1 - \epsilon_g)\sigma(T_w^4 - T_o^4) \tag{11.18}$$

Since, for large fully developed fires, ϵ_g is near 1 or $T_w \approx T_g$, then it follows that

$$\dot{q}_r = A_o \sigma (T^4 - T_o^4) \tag{11.19}$$

and shows that the opening acts like a blackbody. This blackbody behavior for the vents has been verified, and is shown in Figure 11.10 for a large data set of crib fires in enclosures of small scale with H up to 1.5 m [17].

The total heat losses in a fully developed fire can then be approximated as

$$\dot{q} = \dot{q}_w + \dot{q}_r = h_k A(T - T_o) + A_o \sigma (T^2 + T_o^2)(T + T_o)(T - T_o) \tag{11.20}$$
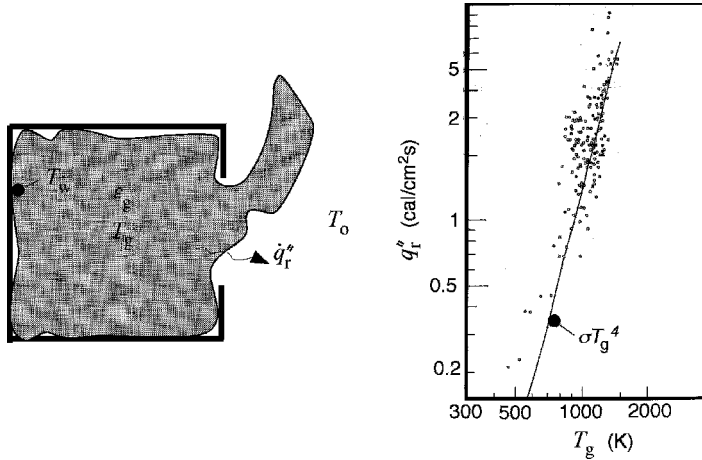
Figure 11.10   Radiation from the compartment vent [17]

11.4   Fuel Behavior

A material burning in an enclosure will depart from its burning rate in normal air due to thermal effects of the enclosure and the oxygen concentration that controls flame heating. Chapter 9 illustrated these effects in which Equation (9.73) describes 'steady' burning in the form:

$$\dot{m}'' = \frac{\dot{q}''}{L} \qquad (11.21)$$

If the fuel responds fast to the compartment changes, such a 'quasi-steady' burning rate model will suffice to explain the expenditure of fuel mass in the compartment. The fuel heat flux is composed of flame and external (compartment) heating. The flame temperature depends on the oxygen mass fraction (Y_{O_2}), and external radiant heating depends on compartment temperatures.

11.4.1   Thermal effects

The compartment net heat flux received by the fuel within the hot upper layer for the blackbody wall and fuel surfaces can be expressed from Equation (11.13) as

$$\dot{q}_r'' = \epsilon_g \sigma_g (T_g^4 - T_v^4) + (1 - \epsilon_g)\sigma(T_w^4 - T_v^4) \qquad (11.22)$$

where T_v is the vaporization temperature of the fuel surface. For fuel in the lower layer, an appropriate view factor should reduce the flux given in Equation (11.22).
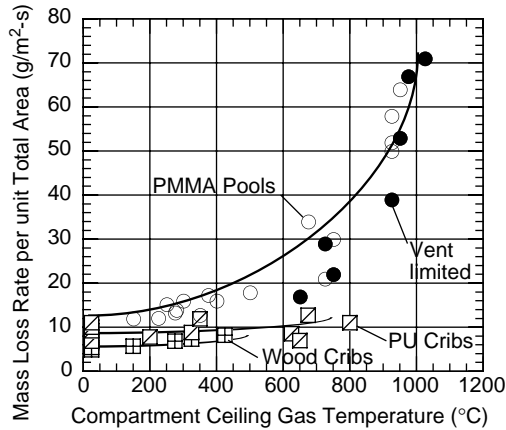
Figure 11.11   Compartment thermal effect on burning rate for wood cribs and pool fire

The quasi-steady maximum burning rate is illustrated in Figure 11.11 for wood cribs and PMMA pool fires under various fuel loading and ventilation conditions [18,19]. The cribs represent fuels controlled by internal combustion effects and radiant heat transfer among the sticks. The pool fires shown in Figure 11.11 are of small scale and have low absorptivity flames. Consequently, the small pools represent a class of fuels that are very responsive to the thermal feedback of the compartment. In general, the small-scale 'pool' fires serve to represent other fuel configurations that are equally as responsive, such as surfaces with boundary layer or wind-blown flames. The crib and pool fire configurations represent aspects of realistic building fuels. They offer two extremes of fuel sensitivity to compartment temperature.

11.4.2   Ventilation effects

As the vent is reduced, mixing will increase between the two layers and the oxygen feeding the fire will be reduced, and the burning rate will correspondingly be reduced. This is shown for some of the data in Figure 11.11 and represents ventilation-controlled burning. Figure 11.12 shows more dramatic effects of ventilation for experimental heptane pool fires in a small-scale enclosure [20]. These experiments included the case of a single ceiling vent or two equal-area upper and lower wall vents. For vent areas below the indicated flame extinction boundary, the fire self-extinguishes. For a fuel diameter of 95 mm, the mass loss rate associated with the ceiling vent was much lower than the wall vent case. The air supply differences indicated by Equations (11.5) and (11.6) suggest that the fuel mass loss rate for the ceiling vent case was limited by air flow.
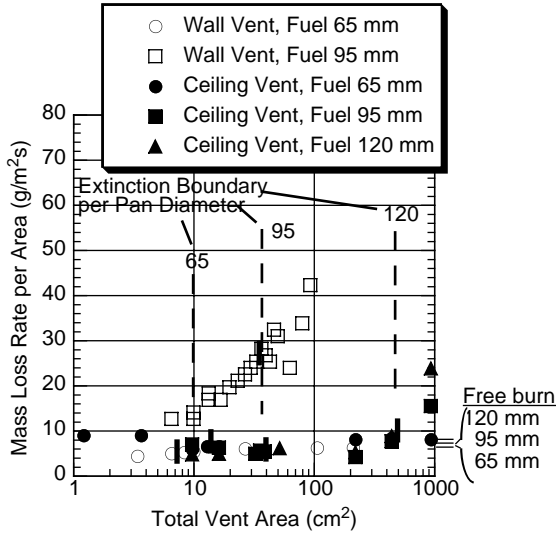
Figure 11.12   Ventilation-controlled burning for ceiling and wall vents [20]

11.4.3   Energy release rate (firepower)

The energy release rate of the fire in a compartment may occur within the compartment, and outside due to normal flame extension or insufficient air supply to the compartment. The energy release rate has been commonly labeled as the heat release rate (HRR); herein the term 'firepower' is fostered, as that is the common term adopted in energy applications. Moreover, the energy associated with chemical reaction is not heat in strict thermodynamic terminology. However, it is recognized that the fire community usage is the 'heat release rate'. Nevertheless, the important factor in compartment fire analysis is to understand the conditions that allow for burning within and outside a compartment. The heat of the flames and smoke causes the fuel to vaporize at a mass flow rate, $\dot{m}_F$. While all of the fuel may eventually burn, it may not necessarily burn completely in the compartment. This depends on the air supply rate. Either all of the fuel is burned or all of the oxygen in the incoming air is burned. That which burns inside gives the firepower within the enclosure. Thus, the firepower within the enclosure is given as

$$\dot{Q} = \begin{cases} \dot{m}_F \Delta h_c, & \phi < 1 \\ \dot{m}_{air} \Delta h_{air}, & \phi \geq 1 \end{cases} \tag{11.23}$$

where $\dot{m}_{air}$ is the mass flow rate of air supplied to the compartment and Δh_{air} is the heat of combustion per unit mass of air, an effective constant for most fuels at roughly 3 kJ/g air. The firepower is based on burning all of the gaseous fuel supplied or all of the air. The equivalence ratio, ϕ, determines the boundary between the fuel-lean and

fuel-rich combustion regimes:

$$\phi = \frac{s\dot{m}_F}{\dot{m}_{air}} \quad (11.24)$$

where s is the stoichiometric air to fuel ratio. Stoichiometry is generally not obvious for realistic fuels as they do not burn completely. However, s can be computed from

$$s = \frac{\Delta h_c}{\Delta h_{air}} \quad (11.25)$$

where Δh_c is the heat of combustion (the chemical heat of combustion, as given in Table 2.3).

It is important to distinguish between the mass loss or supply rate of the fuel and its burning rate within the compartment. The mass loss rate in contrast to Equation (11.23) is given as

$$\dot{m}_F = \begin{cases} \dot{m}_{F,b}'' A_F, & \phi < 1 \\ \dfrac{\dot{m}_{air}}{s} + \dfrac{F\dot{q}_r''}{L}, & \phi \geq 1 \end{cases} \quad (11.26)$$

where $\dot{m}_{F,b}''$ is the fuel burn flux, A_F is the available fuel area, and $F\dot{q}_r$ is the view-factor-modified net radiant flux received (Equation (11.22)). The actual area burning in a ventilation controlled fire ($\phi > 1$) would generally be less than the available area, as suggested by

$$\frac{\dot{m}_{air}}{s} = \dot{m}_{F,b}'' A_{F,b} \quad (11.27)$$

A typical transition to behavior of a ventilation-controlled fire begins with excess air as the fire feeds on the initial compartment air, but then is limited by air flow at the vent. As a consequence the fire can move to the vent and withdraw as the fuel is consumed. This might lead to two areas of 'deep' burning if the fire is extinguished before complete burnout.

11.5   Zone Modeling and Conservation Equations

The above discussion lays out the physics and chemical aspect of the processes in a compartment fire. They are coupled phenomena and do not necessarily lend themselves to exact solutions. They must be linked through an application of the conservation equations as developed in Chapter 3. The ultimate system of equations is commonly referred to as 'zone modeling' for fire applications. There are many computer codes available that represent this type of modeling. They can be effective for predictions if the
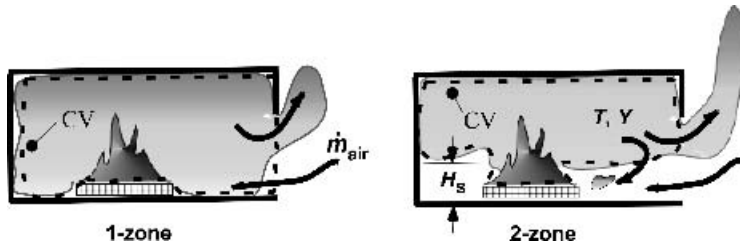
Figure 11.13   Control volume for conservation equations

fire processes are completely and accurately represented. Complete finite difference modeling of the fundamental equations is a step more refined than zone modeling, and it also has limitations, but will not be discussed here. Zone modeling is no more than the development of the conservation laws for physically justifiable control volumes. The control volume is principally the hot gas layer of the compartment fire. The fire is embedded within this volume. Figure 11.13 can be used to define a control volume for either the two-zone or one-zone approach. In the former, the lower layer would constitute another control volume. For simplicity, the one-zone model will only be considered here for illustration. This limited development is simply to present the methodology and demonstrate the basis for empirical correlations to follow.

11.5.1   Conservation relationships

Principally, conservation of energy for the compartment provides the important relationship to establish the extent of thermal feedback to the fuel. Conservation of mass and oxygen provide additional support equations. The 'process' relationships, given previously, establish the important transport rates of mass and energy. These 'constitutive' relationships may not always be complete enough to describe all fire scenarios.

The conservation equations can be developed from Chapter 3. They are listed below:

1. *Mass.* For the one-zone model with a perfect gas using Equation (3.15), the conservation of mass can be written as

$$-\frac{pV}{RT^2}\frac{\mathrm{d}T}{\mathrm{d}t} + \dot{m} = \dot{m}_{\mathrm{air}} + \dot{m}_{\mathrm{F}} \tag{11.28}$$

The conservation of oxygen for the mass fraction designation by Y follows from Equation (3.22).

2. *Oxygen*

$$\frac{\mathrm{d}(mY)}{\mathrm{d}t} + \dot{m}Y - \dot{m}_{\mathrm{air}}(0.233) = -\frac{0.233s\dot{Q}}{\Delta h_{\mathrm{c}}} \tag{11.29}$$

Under steady conditions, or where the transient term is negligible, this is simply

$$Y = \frac{0.233(1 - \phi)}{1 + \phi/s} \quad \text{for } \phi \leq 1 \tag{11.30}$$

and

$$Y = 0 \quad \text{for the (global) equivalence ratio, } \phi > 1$$

The energy equation follows from Equation (3.45) where the 'loss' terms are grouped to include both heat and enthalpy transport rates as $\dot{Q}_{\text{l}}$.

3. *Energy*

$$c_v \frac{\mathrm{d}(mT)}{\mathrm{d}t} = \frac{c_v V}{R} \frac{\mathrm{d}p}{\mathrm{d}t} = \dot{Q} - \dot{Q}_{\text{l}} \tag{11.31}$$

The transient term can be neglected in most cases, but any sudden change in the energy will result in a pressure change. This can be responsible for 'puffing' effects seen in compartment fires, especially when the burning is oscillatory.

11.5.2 *Dimensionless factors in a solution*

By normalizing the steady equation with the air flow rate and representing all of the losses as linear in T (Equation (11.31)), the temperature rise can be solved as

$$T - T_{\text{o}} = \frac{\dot{Q}/(c_p \dot{m}_{\text{air}})}{x_{\text{o}} + x_{\text{w}} + x_{\text{r}}} \tag{11.32}$$

The dimensionless x-loss factors are parameters that effect temperature, and occur in modified forms in many correlations in the literature for compartment fire temperature.

1. *Flow-loss factor.* The flow factor, x_{o}, is the ratio of out-flow to airflow:

$$x_{\text{o}} = 1 + \frac{\dot{m}_{\text{F}}}{\dot{m}_{\text{air}}} = 1 + \frac{\phi}{s} \tag{11.33}$$

and is approximately 1 for $\phi < 1$ since s ranges from 3 to 13 for charring to liquid fuels respectively.

2. *Wall-loss factor.* The wall-loss factor, x_{w}, is given in terms of the compartment heat transfer surface area, A, and the overall heat transfer coefficient, h, as given by Equation (11.17):

$$x_{\text{w}} = \frac{hA}{\dot{m}_{\text{air}} c_p} \geq \frac{hA}{k_{\text{o}} c_p A_{\text{o}} \sqrt{H_{\text{o}}}} \tag{11.34}$$

Here, the maximum air flow rate could be inserted per Equation (11.7). In general, h depends on convection (h_{c}), radiation (h_{r}) and conduction into the walls (h_{k}). Their typical values range as $h_{\text{c}} \sim 10$–30, $h_{\text{r}} \sim 5$–100 and $h_{\text{k}} \sim (k\rho c/t)^{1/2} \sim 5$–$60$ W/m^2 K; consequently, $h \sim 1$ to 100 W/m^2 K is a typical range expected. It is important to note

that the wall conductance will decrease with time for thick walls, leading to an increase in temperature.

3. *Vent-radiation factor.* As shown by Figure 11.10, the radiation flux from the vent is reasonably represented as a blackbody at the gas temperature, T. Thus, the vent radiation loss can be estimated as

$$x_r = \frac{\dot{q}_{r,o}''}{\dot{m}_{air} c_p (T - T_o)}$$

$$\geq \frac{\sigma(T^4 - T_o^4) A_o}{c_p k_o A_o \sqrt{H_o}(T - T_o)} \approx \frac{\sigma T^3}{c_p k_o \sqrt{H_o}} \quad \text{for } T_o/T \text{ small} \qquad (11.35)$$

This factor might range from roughly 10^{-2} to 10^{-1} for T ranging from 25 to 1200 °C respectively. It is the least significant of the three factors.

11.6   Correlations

While computer models exist to solve for many aspects of compartment fires, there is nothing more valuable than the foundation of experimental results. Empirical correlations from such experimental data and based on the appropriate dimensionless groups have been developed by many investigators. These can be very useful to the designer and investigator. As with computer models, these correlations can also be incomplete; they may not have tested over a sufficient range of variables, they may leave out important factors and they are still usually specific to the fuels and their configuration. Nevertheless, they are very powerful, in their algebraic or graphical simplicity, and in their accuracy. Some will be listed here. The SFPE guide addressing fully developed enclosure fires is an excellent source of most correlations [2].

11.6.1   Developing fires

The developing fire applies up to flashover, and therefore might apply to an average temperature in the upper layer of 600 °C, at most. McCaffrey, Quintiere and Harkleroad [21] developed a well-known correlation for this domain known as the MQH correlation. The MQH correlation was developed from a large database for compartment fires ranging in scale from 0.3 to 3 m high, and with fuels centered on the floor [21]. Other investigators have followed the form of this correlation for floor fires near a wall, in a corner and for burning wall and ceiling linings [22–25]. This correlation takes the form of Equation (11.32), but as a power law. The dimensionless groups that pertain are dimensionless mass and energy flow rates of the form:

$$m^* = \frac{\dot{m}}{\rho_o \sqrt{g} A_o \sqrt{H_o}} \qquad \text{and} \qquad Q^* = \frac{\dot{Q}}{\rho_o c_p T_o \sqrt{g} A_o \sqrt{H_o}} \qquad (11.36)$$

The dimensionless fuel supply and air inflow rate can be described, accordingly, as m_F^* and m_A^* respectively. The entrainment rate depends on the height over which entrainment

Table 11.3   Values of C_T for different fire configurations

Fire Configuration	C_T	Source
Discrete, centered	480	McCaffrey et al.[21]
	686	Azhakesan et al.[23]
Discrete, against wall	615	Mowrer et al.[22]
Discrete, in corner	804	Azhakesan et al.[23]
	856	Mowrer et al.[22]
Linings, wall only	1200	Azhakesan et al. [25]
	1060–1210	Karlsson [24]
Linings, wall and ceiling	1000	Azhakesan et al. [25]
	940	Karlsson [24]

occurs H_s, and on the fire configuration. This factor is simply represented here by G. Thus, the entrainment rate and air flow rate might functionally be represented as

$$m_A^* = \text{function} \left(G, \frac{H_s}{H_o} \right) \tag{11.37}$$

Eliminating the H_s dependence by Equation (11.4), the temperature of the hot layer can generally be functionally expressed

$$\frac{T}{T_o} = \text{ function} \left(Q_o^*, Q_w^*, m_F^*, G \right) \tag{11.38}$$

The MQH correlation for the layer temperature rise has found the empirical fit to data:

$$\Delta T = C_T(G, m_F^*) Q_o^{*^{2/3}} Q_w^{*^{-1/3}} \tag{11.39}$$

where Q_o^* from Equation (11.36) has $\dot{Q}$ as the firepower, and Q_w^* has $\dot{Q}$ taken as $h_k A T_o$ from Equations (11.10) and (11.11). These Q^* values correspond to x_o and x_w in Equation (11.32); i.e.

$$Q_o^* = \frac{\dot{Q}}{\rho_\infty c_p T_\infty \sqrt{g} A_o \sqrt{H_o}} \qquad \text{and} \qquad Q_w^* = \frac{h_k A}{\rho_\infty c_p \sqrt{g} A_o \sqrt{H_o}}$$

C_T is an empirical constant that appears to increase as the entrainment rate decreases, as shown from the evidence in Table 11.3. Also from Equation (11.32), the temperature will decrease as the dimensionless fuel supply rate increases. Equation (11.39) holds for the overventilation regime, and therefore it should not be used at a point where $\dot{m}_F/\dot{m}_{air} = 1/s$ or $\phi = 1$ without at least modifying Q_o^*.

Figure 11.14 shows the original MQH data fit and Figures 11.15 and 11.16 show results for compartment lining material fires. Various lining materials were used and the firepower was measured by oxygen calorimetry. Departure from the linear slope behavior marks the onset of the ventilation-limited fires where the correlation based on the total firepower, within and outside the compartment, does not hold. The results for the lining fires also show the importance of the m_F^* factor omitted from the simple MQH correlation.
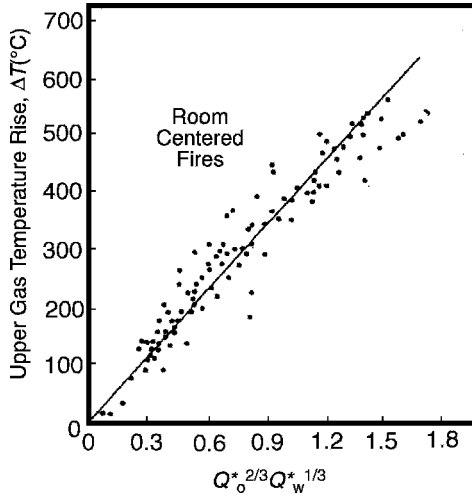
Figure 11.14   MQH correlation for discrete floor-centered fires [21]

11.6.2   *Fully developed fires*

The fully developed fire is defined as the state where all of the fuel that can get involved is involved. It does not necessarily mean that all of the fuel is burning, since the lack of air would prevent this. In most building occupancies, the fuel load is high enough to lead to a significant fire that can threaten the structure. This means a significantly high temperature is produced for a long time. Hence, many fully developed fire studies have been motivated to establish the thermal characteristics needed to assess the structural fire resistance. Consequently, these studies have aimed to establish correlations for gas temperature and the fuel burning rate (or more exactly, its mass loss rate). The latter can
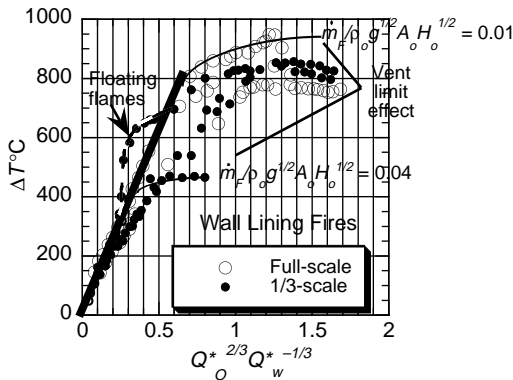

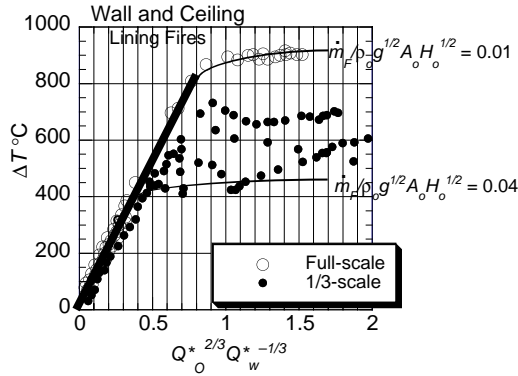**Figure 11.15**   Temperature for wall lining fires [25]

Figure 11.16 Temperatures for wall and ceiling lining fires [25]

then give the fire duration for a given fuel mass loading in the occupancy. Occupancy studies have been performed from time to time to give typical fuel loadings (usually in wood equivalent), which may range from 10 to 50 kg/m^2 (floor area).

One aspect of fully developed fires that will not be addressed here is their production of combustion products. When compartment fires become ventilation-limited, they burn incompletely, and can spread incomplete products such as CO, soot and other hydrocarbons throughout the building. It is well established that the yield of these incomplete products goes up as the equivalence ratio approaches and exceeds 1. More information on this issue can be found in the literature [1].

Fully developed fire studies have been performed over a range of fuel loadings and ventilation conditions, but primarily at scales smaller than for normal rooms. Also the fuels have been idealized as wood cribs or liquid or plastic pool fires. The results have not been fully generalized. The strength of the dimensionless theoretical implication of Equation (11.38) suggests that, for a given fuel, the fully developed, ventilation-limited fire should have dependences as

$$\frac{T}{T_o} = \text{ function } \left(Q_w^*, m_F^*, G\right) \tag{11.40}$$

where Q_o^* has been eliminated since $\dot{Q}$ depends only on the air flow rate from Equation (11.23), and that depends on the temperature from the flow equation (e.g. Equation (11.5)). Thus, for a given burning configuration (represented in terms of G),

$$T \sim \frac{h_k A}{\rho_\infty c_p \sqrt{g} A_o \sqrt{H_o}}, \quad \frac{\dot{m}_F}{\rho_\infty \sqrt{g} A_o \sqrt{H_o}} \tag{11.41}$$

From Equation (11.21) and recognizing that the heat flux to the fuel depends on the flame and compartment temperatures, it follows that

$$\dot{m}_F \sim \frac{A_F \dot{q}''(T)}{L} \tag{11.42a}$$

or

$$m_F^* \approx \frac{\dot{m}_F}{\rho_\infty \sqrt{g} A_o \sqrt{H_o}} \sim \left(\frac{A_F \sigma T_\infty^4}{\rho_\infty \sqrt{g} A_o \sqrt{H_o} L} \right) \left(\frac{\dot{q}''(T)}{\sigma T_\infty^4} \right) \tag{11.42b}$$

By rearrangement of these functional dependencies, it follows for a given fuel (L) that

$$T \text{ and } \frac{\dot{m}_F}{\rho_\infty \sqrt{g} A_o \sqrt{H_o}} \sim \frac{A}{A_o \sqrt{H_o}}, \frac{A_F}{A} \tag{11.43}$$

Investigators have developed correlations for experimental data in this form.

Law developed a correlation for the extensive Conseil International du Bâtiment (CIB) test series [17] involving wood cribs that covered most of the compartment floor [26]. The test series also addressed the effect of compartment shape by varying its width (W) and depth (D). The correlation for the maximum temperature was given as

$$T_{max} = 6000 \left(\frac{1 - e^{-0.1\Omega}}{\sqrt{\Omega}} \right) (^\circ C) \qquad \Omega = \frac{A}{A_o \sqrt{H_o}} \quad \text{in m}^{-1/2} \tag{11.44}$$

Most of the CIB tests involved crib arrangements having A_F/A of mostly 0.75 [2]; therefore, leaving this parameter out of the correlation may be justified. However, for low fuel loadings, Law recommended that the maximum temperature be reduced accordingly:

$$T = T_{max} \left(1 - e^{-0.05\Psi} \right) (^\circ C), \qquad \Psi = \frac{m_F}{\sqrt{A A_o}} \quad \text{in kg/m}^2 \tag{11.45}$$

where m_F is the fuel load in kg.

The mass loss rate is correlated as

$$\dot{m}_F = 0.18 A_o \sqrt{H_o} \left(\frac{W}{D} \right) (1 - e^{-0.036\Omega}) \quad \text{in kg/s}$$

$$\text{for } \frac{\dot{m}_F}{A_o \sqrt{(H_o)}} \left(\frac{D}{W} \right)^{1/2} < 60 \text{ kg/s m}^{5/2} \tag{11.46}$$

The data corresponding to these correlations are shown in Figures 11.17 and 11.19.

The CIB tests consisted of compartments with heights ranging from 0.5, 1.0 and 1.5 m with dimension ratios of $D/H, W/H, H/H$ coded as data sets: 211, 121, 221 and 441. A total of 321 experiments were conducted in still air conditions. The wood crib fuel loading ranged from 10 to 40 kg/m^2 with stick spacing to stick thickness ratios of $\frac{1}{3}$, 1 and 3. The data are plotted in Figures 11.17 and 11.19. The compartment surface area, A, excludes the floor area in the plot variables.

An alternative plotting format was used by Bullen and Thomas [6] for the mass loss rate, which shows the effect of fuel type in Figure 11.18. These data include an extensive compilation by Harmathy [27] for wood crib fuels (including the CIB data). Here the fuel area is included, but the compartment area is omitted. This shows the lack of
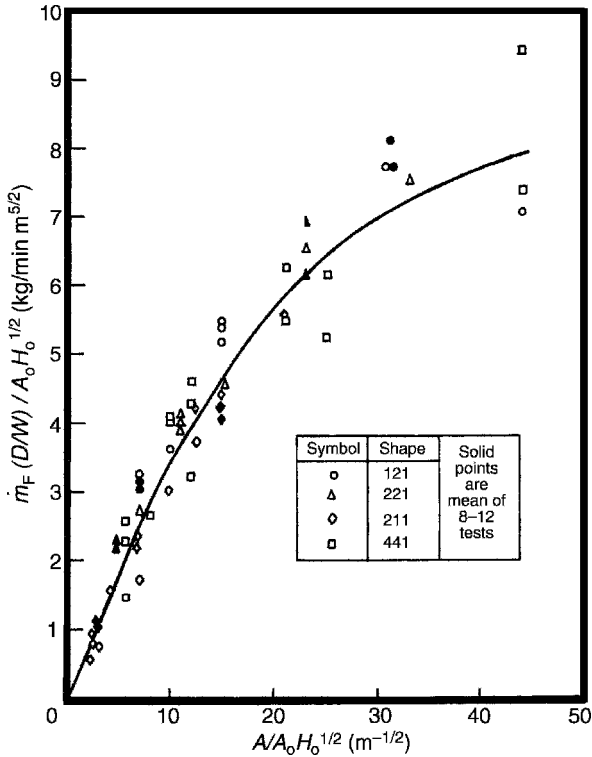
Figure 11.17   Normalized mass loss rate for CIB data [17]

completeness of the correlations. However, they are still invaluable for making accurate estimates for fully developed fires. Harmathy gives a fit to the wood crib data in Figure 11.18 as

$$\dot{m}_F = \begin{cases} (0.0062 \text{ kg/m}^2 \text{ s})A_F, & \dfrac{\rho_\infty \sqrt{g}A_o\sqrt{H_o}}{A_F} \geq 0.263 \text{ kg/s} \\[3mm] 0.0263\rho_\infty\sqrt{g}A_o\sqrt{H_o}, & \dfrac{\rho_\infty\sqrt{g}A_o\sqrt{H_o}}{A_F} < 0.263 \text{ kg/s} \end{cases} \tag{11.47}$$

The latter equation corresponds to the CIB data and Law's correlation for large $A/(A_o\sqrt{H_o})$, i.e. ventilation-limited fires. At the asymptote for large $A/(A_o\sqrt{H_o})$ from Figure 11.18, the CIB results are for $D = W$, roughly

$$\dot{m}_F \approx 0.13A_o\sqrt{H_o} \quad \text{kg/s}$$

and for Harmathy with $\rho_\infty = 1.16$ kg/m^3,

$$\dot{m}_F = 0.086 \, A_o\sqrt{H_o} \text{ kg/s}$$

with A_o in m^2 and H_o in m. These differences show the level of uncertainty in the results.
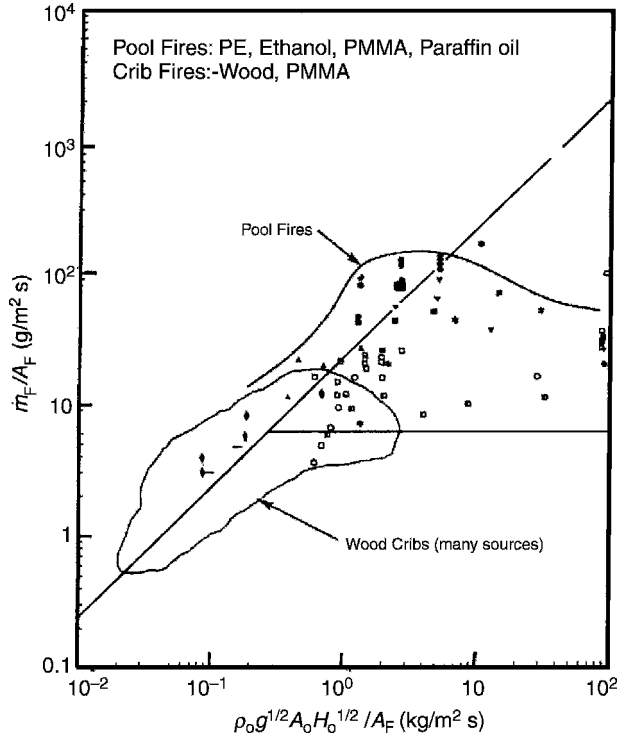
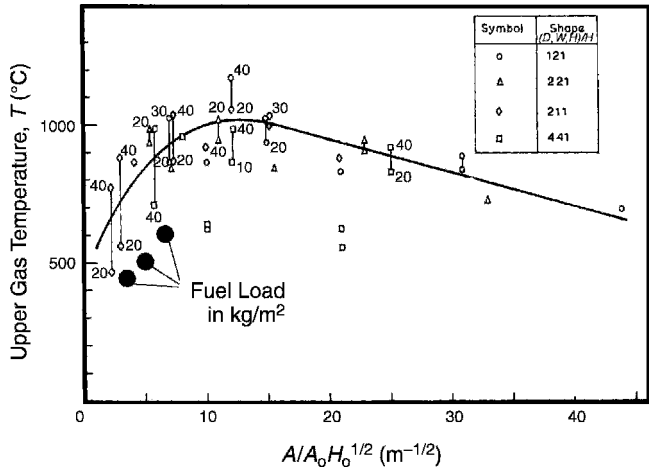**Figure 11.18**   Fuel mass loss rate in fully developed fires [6]

Figure 11.19   CIB compartment fully developed temperature [17]

11.7   Semenov Diagrams, Flashover and Instabilities

The onset of flashover as considered here is induced by thermal effects associated with the fuel, its configuration, the ignition source and the thermal feedback of the compartment. Several fire growth scenarios will be considered in terms of Semenov diagrams (Chapters 4 and 9) portraying the firepower $\dot{Q}$ and the loss rates $\dot{Q}_l$ as a function of compartment temperature. According to Equation (11.31), a 'thermal runaway' will occur at the critical temperature where $\dot{Q} = \dot{Q}_l$ and the two curves are tangent. The developing fire occurs for $\phi < 1$ and the result of a critical event will lead to a fully developed fire with $\phi > 1$ likely. Four scenarios will be examined:

1. Fixed fire area, representative of a fully involved fuel package, e.g. chair, crib, pool fire.

2. Ignition of a second item, representing an initial fire (e.g. chair, liquid spill) and the prospect of ignition of an adjoining item.

3. Opposed flow flame spread, representing spread on a horizontal surface, e.g. floor, large chair, mattress, etc.

4. Concurrent flow flame spread, representing vertical or ceiling spread, e.g. combustible linings.

In all of these scenarios, up to the critical condition (flashover),

$$\phi < 1 \qquad \text{and} \qquad \dot{Q} = \dot{m}_F'' A_F \Delta h_c \qquad (11.48)$$

Here A_F will be taken to represent the projected external fuel surface area that would experience the direct heating of the compartment. From Equation (11.21), accounting approximately for the effects of oxygen and temperature, and distribution effects in the compartment, the fuel mass flux might be represented for qualitative considerations as

$$\dot{m}_F'' = \dot{m}_{F,o}''(1 - \gamma_o \phi) + \frac{\gamma_T \sigma(T^4 - T_o^4)}{L} \qquad (\phi < 1) \qquad (11.49)$$

where $\dot{m}_{F,o}''$ refers to the burning flux in normal air. The distribution factors, γ_o and γ_T, are estimated to range from about 0.5 to 1 as the smoke layer descends and mixing causes homogeneous properties in the compartment. The oxygen distribution factor is very approximate and is introduced to account for the oxygen in the flow stream in the lower gas layer. The thermal parameter, γ_T, represents a radiation view factor. For all of these scenarios, the effect of oxygen on the burning rate is expected to be small, as the oxygen concentration does not significantly decrease up to flashover. The loss rate is given as, from Equations (11.31) and (11.32),

$$\dot{Q}_l = \dot{m}_{air} c_p [x_o + x_w(t) + x_r(T)](T - T_o) \qquad (11.50)$$

The loss rate is nearly linear in T for low temperatures, and can depend on time, t, as well. Since T is a function of time, the normal independent variable t should be
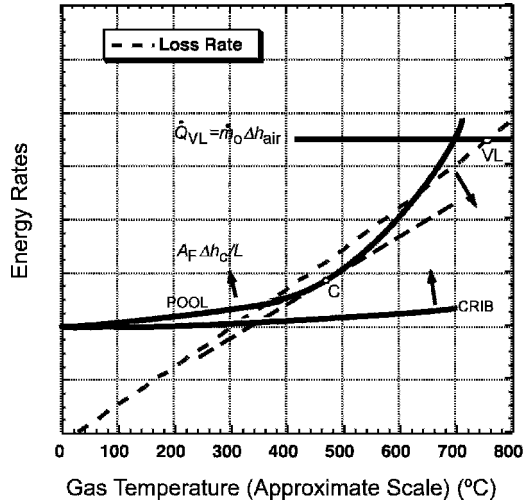
Figure 11.20   Fixed area fire

considered as dependent since the inverse function $t = t(T)$ should be available, in principle. This functional dependence will not be made explicit in the following.

11.7.1   Fixed area fire

Figure 11.20 shows the behavior of the energy release and losses as a function of compartment temperature (Semenov diagram) for fuels characteristic of cribs and 'pool' fires (representative of low flame absorbing surface fuels, e.g. walls). As the loss curve decreases due to increasing time or increasing ventilation factor ($A/A_o\sqrt{H_o}$), a critical condition (C) can occur. The upward curvature and magnitude of the energy release rate increases with $A_F\Delta h_c/L$. Thomas *et al*. [4] has estimated the critical temperatures to range from about 300 to 600 °C depending on the values of L. Thus, liquid fuels favor the lower temperature, and charring solids favor the higher. An empirical value of 500 °C (corresponding to 20 kW/m^2 blackbody flux) is commonly used as a criterion for flashover. The type of flashover depicted here is solely due to a fully involved single burning item. A steady state condition that can be attained after flashover is the ventilation-limited (VL) branch state shown in Figure 11.20 in which $\dot{Q} = \dot{m}_o\Delta h_{air}$ for $\phi = 1$. It can be shown that the state of oxygen at the critical condition is always relatively high, with $\phi < 1$. This clearly shows that oxygen depletion has no strong effect. Also, Thomas *et al*. [4] show that the burning rate enhancement due to thermal feedback at the critical condition is only about 1.5, at most.

11.7.2   Second item ignition

Figure 11.21 depicts the behavior for a neighboring item when becoming involved due to an initiating first fire. The first fire could be a fixed gas burner as in a test or a fully
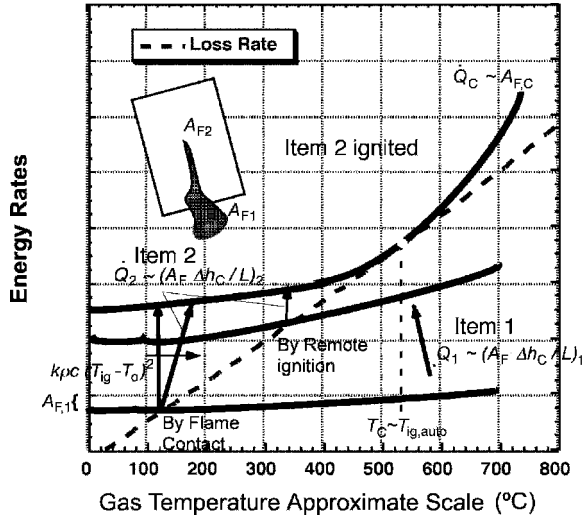
Figure 11.21   Second item ignited

involved fuel, $A_{F,1}$. For illustrative purposes, assume the second item has similar properties to $A_{F,1}$, and A_F represents the combined area after ignition. Ignition of the second item is possible if the material receives a heat flux higher than its critical flux for ignition. It can possibly receive heat by flame heating ($\dot{q}_f''$) and heating from the compartment. The critical condition for ignition occurs at a balance between the compartment heating and the objects heat loss estimated by

$$\dot{q}_f'' + \gamma_T \sigma(T^4 - T_o^4) = \sigma(T_{ig}^4 - T_o^4) + h_c(T_{ig} - T_o) \tag{11.51}$$

For remote ignition under autoignition conditions, direct flame heating is small or zero, so the critical compartment temperature needs to be greater than or equal to the autoignition temperature, e.g. about 400–600 °C for common solid fuels.

For ignition by flame contact (to a wall or ceiling), the flame heat flux will increase with D_F, the flame thickness of the igniter, estimated by

$$\dot{q}_f'' \sim 1 - \exp(-\kappa D_F) \geq 30 \text{ kW/m}^2, \text{ usually} \tag{11.52}$$

The exposed area of the second item exposed ($A_{F,2}$) depends on the flame length (z_f) and its diameter.

For the second item ignition to lead to flashover, the area involved must equal or exceed the total critical area needed for the second item. The time for ignition depends inversely on the exposure heat flux (Equation (11.51)). Figure 11.21 shows the behavior for ignition of the second item, where $A_{F,1}$ is the fixed area of the first item and $A_{F,C}$ is the critical area needed. The energy release rate of both fuels controls the size of the 'jump' at criticality and depends directly on $A_F \Delta h_c / L$. No flashover will occur if the 'jump' in energy for the second item is not sufficient to reach the critical area of fuel, $A_{F,C}$. The time to achieve the jump or to attain flashover is directly related to the fuel property,

$k\rho c(T_{ig} - T_o)^2$. For flame contact, the piloted ignition temperature applies and the ignition time is expected to be small ($\sim$ 10–100 s).

11.7.3 Spreading fires

The flame spread rate can be represented in terms of the pyrolysis front (x_p) from Equation (8.7a):

$$v = \frac{dx_p}{dt} \approx \frac{\delta_f}{t_{ig}} \tag{11.53}$$

where δ_f is a flame heating length. In opposed flow spread into an ambient flow of speed u_o, this length is due to diffusion and can be estimated by Equation (8.31) as $\delta_{f,opposed} \sim (k/\rho c)_o / u_o$. This length is small ($\sim$ 1 mm) under most conditions, and is invariant in a fixed flow field. However, in concurrent spread, this heating length is much larger and will change with time. It can be very dependent on the nature of the ignition source since here $\delta_f = z_f - x_p$. In both cases, the area of the spreading fire (neglecting burnout) grows in terms of the velocity and time as $(vt)^n$, with n ranging from 1 to 2.

The surface flame spread cases are depicted in Figure 11.22. In opposed flow spread, the speed depends on the ignition time, which decreases as the compartment heats the fuel surface. After a long time, $T_{surface} = T_{ig}$ and the growth curves approach a vertical asymptote. Consider the initial area ignited as $A_{F,i}$ and $A_{F,C}$ as the critical area needed for a fixed area fire. The area for a spreading fire depends on the time and therefore T as well. For low-density, fast-responding materials, the critical area can be achieved at a compartment temperature as low as the ignition temperature of the material.
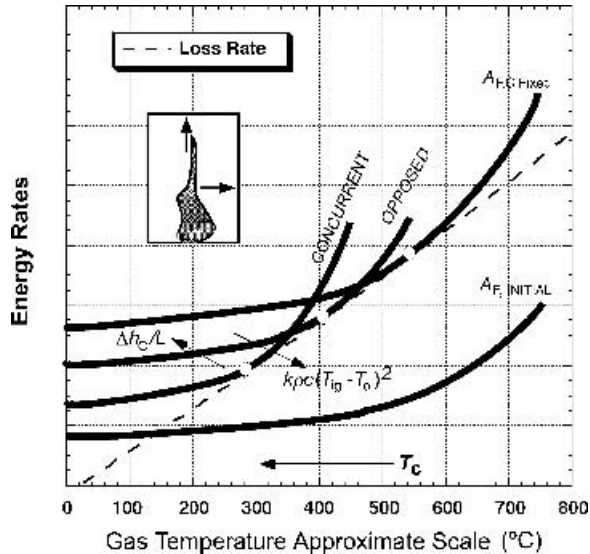

Figure 11.22 Surface spread fire growth

For concurrent spread, the growth rate can be much faster, and therefore the critical condition can be reached at lower compartment temperatures. The dependence of the concurrent flame spread area on both $\dot{Q}$ and the surface temperature of the material make this spread mode very feedback sensitive.

The Semenov criticality diagrams for fire growth are useful to understand the complex interactions of the fire growth mechanisms with the enclosure effects. These diagrams can be used qualitatively, but might also be the bases of simple quantitative graphical solutions.

References

1. Karlsson, B. and Quintiere, J. G., *Enclosure Fire Dynamics*, CRC Press, Boca Raton, Florida, 2000.
2. *Engineering Guide to Fire Exposures to Structural Elements*, Society of Fire Protection Engineers, Bethesda, Maryland, May 2004.
3. Thomas, P. H., Behavior of fires in enclosures – some recent progress, in 14th International Symposium on Combustion, The Combustion Institute, Pittsburgh, Pennsylvania, 1973, pp. 1007–20.
4. Thomas, P. H., Bullen, M. L., Quintiere, J. G. and McCaffrey, B. J., Flashover and instabilities in fire behavior, *Combustion and Flame*, 1980, **38**, 159–71.
5. Thomas, P. H., Fires and flashover in rooms – a simplified theory, *Fire Safety J.*, 1980, **3**, 67–76.
6. Bullen, M. L. and Thomas, P. H., Compartment fires with non-cellulosic fuels, in 17th International Symposium on *Combustion*, The Combustion Institute, Pittsburgh, Pennsylvania, 1979, pp. 1139–48.
7. Tewarson, A., Some observations in experimental fires and enclosures, Part II: ethyl alcohol and paraffin oil, *Combustion and Flame*, 1972, **19**, 363–71.
8. Kim, K. I., Ohtani, H. and Uehara, Y., Experimental study on oscillating behavior in a small-scale compartment fire, *Fire Safety J.*, 1993, **20**, 377–84.
9. Takeda, H. and Akita, K., Critical phenomenon in compartment fires with liquid fuels, in 18th International Symposium on *Combustion*, The Combustion Institute, Pittsburgh, Pennsylvania, 1981, 519–27.
10. Quintiere, J. G., McCaffrey, B. J. and Rinkinen, W., Visualization of room fire induced smoke movement in a corridor, *Fire and Materials*, 1978, **12**(1), 18–24.
11. Quintiere, J. G., Steckler, K. D. and Corley, D., An assessment of fire induced flows in compartments, *Fire Sci. Technol.*, 1984, **4**(1), 1–14.
12. Emmons, H. W., Vent flows, in *The SFPE Handbook of Fire Protection Engineering*, 2nd edn (eds P.J. DiNenno *et al.*), Section 2, Chapter 5, National Fire Protection Association, Quincy, Massachusetts, 1995, pp. **2**-40 to **2**-49.
13. Epstein, M., Buoyancy-driven exchange flow through small openings in horizontal partitions, *J. Heat Transfer*, 1988, **110**, 885–93.
14. Steckler, K. D., Quintiere, J. G. and Rinkinen, W. J., Flow induced by fire in a room, in 19th International Symposium on *Combustion*, The Combustion Institute, Pittsburgh, Pennsylvania, 1983.
15. Rockett, J. A., Fire induced flow in an enclosure, *Combustion Sci. Technol.*, 1976 **12**, 165.
16. Tanaka, T. and Yamada, S., Reduced scale experiments for convective heat transfer in the early stage of fires, *Int. J. Eng. Performanced-Based Fire Codes*, 1999, **1**(3), 196–203.
17. Thomas, P.H. and Heselden, A.J.M., Fully-developed fires in single compartment, a co-operative research programme of the Conseil International du Bâtiment, Fire Research Note 923, Joint Fire Research Organization, Borehamwood, UK, 1972.

18. Quintiere, J. G. and McCaffrey, B. J., *The Burning Rate of Wood and Plastic Cribs in an Enclosure*, Vol. 1, NBSIR 80-2054, National Bureau of Standards, Gaithersburg, Maryland, November 1980.

19. Quintiere, J. G., McCaffrey, B. J. and DenBraven, K., Experimental and theoretical analysis of quasi-steady small-scale enclosure fires, in 17th International Symposium on *Combustion*, The Combustion Institute, Pittsburgh, Pennsylvania, 1979, pp. 1125–37.

20. Naruse, T., Rangwala, A. S., Ringwelski, B. A., Utiskul, Y., Wakatsuki, K. and Quintiere, J. G., Compartment fire behavior under limited ventilation, in *Fire and Explosion Hazards, Proceedings of the 4th International Seminar*, Fire SERT, University of Ulster, Northern Ireland, 2004, pp. 109–120.

21. McCaffrey, B. J., Quintiere, J. G. and Harkleroad, M. F., Estimating room temperatures and the likelihood of flashover using fire test data correlations, *Fire Technology*, May 1981, **17**(2), 98–119.

22. Mowrer, F. W. and Williamson, R B., Estimating temperature from fires along walls and in corners, *Fire Technology*, 1987, **23**, 244–65.

23. Azhakesan, M. A., Shields, T. J., Silcock, G. W. H. and Quintiere, J. G., An interrogation of the MQH correlation to describe centre and near corner pool fires, *Fire Safety Sciences, Proceedings of the 7th International Symposium*, International Association for Fire Safety Science, 2003, pp. 371–82.

24. Karlsson, B., Modeling fire growth on combustible lining materials in enclosures, Report TBVV–1009, Department of Fire Safety Engineering, Lund University, Lund, 1992.

25. Azhakesan, M. A. and Quintiere, J. G., The behavior of lining fires in rooms, in *Interflam 2004*, Edinburgh, 5–7 July 2004.

26. Law, M., A basis for the design of fire protection of building structures, *The Structural Engineer*, January 1983, **61A**(5).

27. Harmathy, T. Z., A new look at compartment fires, Parts I and II, *Fire Technology*, 1972, **8**, 196–219, 326–51.

Problems

11.1 A trash fire occurs in an elevator shaft causing smoke to uniformly fill the shaft at an average temperature of 200 °C.
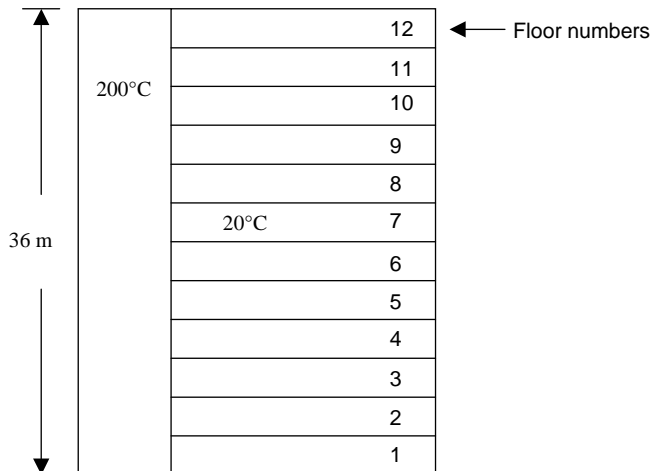
The only leakage from the shaft can occur to the building that is well ventilated and maintained at a uniform temperature of 20 °C. The leak can be approximated as a 2 cm wide vertical slit which runs along the entire 36 m tall shaft.

(a) Calculate the mass flow rate of the smoke to the floors.

(b) What floors receive smoke? Compute neutral plume height.

(c) What is the maximum positive pressure difference between the shaft and the building and where does it occur?

11.2 A 500 kW fire in a compartment causes the smoke layer to reach an average temperature of 400 °C. The ambient temperature is 20 °C. Air and hot gas flow through a doorway at which the neutral plane is observed to be 1 m above the floor. A narrow slit 1 cm high and 3 m wide is nominally 2 m above the floor.
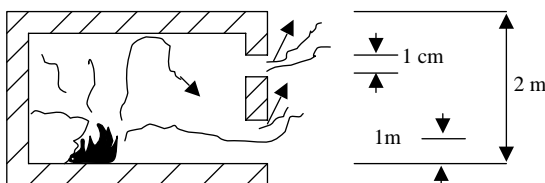

Assume the pressure does not vary over the height of the slit.

(a) Calculate the pressure difference across the slit.

(b) Calculate the mass flow rate through the slit. The slit flow coefficient is 0.7.

11.3 A fire occurs in a 3 m cubical compartment made of 2 cm thick. Assume steady state heat loss through the concrete whose thermal conductivity is 0.2 W/m^2 K. By experiments, it is found that the mass loss rate, $\dot{m}$, of the fuel depends on the gas temperature rise, ΔT, of the compartment upper smoke layer:

$$\dot{m} = \dot{m}_o + \beta(\Delta T)^{3/2}$$

where $\dot{m}_o = 10$ g/s, $\beta = 10^{-3}$ g/sK$^{3/2}$ and $\Delta T = T - T_\infty$. The compartment has a window opening 1 m × 1 m. The heat of combustion for the fuel is 20 kJ/g and ambient air is at 20 °C. Compute the gas temperature rise, ΔT.
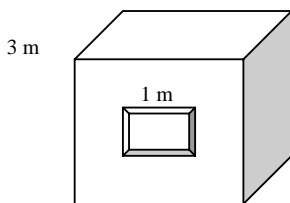

11.4 A room 3 m × 4 m × 3 m high with an opening in a wall 2 m × 2 m contains hexane fuel, which can burn in pools on the floor. The ambient temperature is 25 °C. The heat of combustion for hexane is 43.8 kJ/g. The construction material of the room is an insulator which responds quickly, and thus has a constant effective heat loss coefficient, $h_k = 0.015$ kW/m^{2}K. Use this to compute the overall heat loss to the room.

(a) A pool 0.8 m in diameter is ignited and the flame just touches the ceiling. What is the energy release rate of this fire?

(b) If this fire entrains 10 times stoichiometric air, what is the equivalence ratio for this room fire?

(c) What is the average gas temperature of the hot layer for the fire described in (a)?

(d) Flashover is said to commence if the temperature rise of the gas layer is 600 °C. At this point, more of the hexane can become involved. What is the energy release rate for this condition?

(e) What is the flame extent for the fire in (d)? Assume the diameter of the pool is now 1 m.

(f) Based on a room average gas temperature of 625 °C, what is the rate of air flow through the opening in g/s? Assume the windowsill opening is above the height of the hot gas layer interface of the room.

(g) What is the equivalence ratio for the onset of flashover where the gas temperature is 625 °C? (*Hint*: the heat of combustion per unit mass of air utilized is 3.0 kJ/g.)

(h) What is the energy release rate when the fire is just ventilation-limited, i.e. the equivalence ratio is one? Assume the air flow rate is the same as that at the onset of flashover as in (f).

(i) What is the fuel production rate when the fire is just ventilation-limited?

11.5 A fire in a ship compartment burns steadily for a period of time. The average smoke layer achieves a temperature of 420 °C with the ambient temperature being 20 °C. The compartment is constructed of 1 cm thick steel having a thermal conductivity of 10 W/m^2 K. Its open doorway hatch is 2.2 m high and 1.5 m wide. The compartment has an interior surface area of 60 m^2. The fuel stoichiometric air to fuel mass ratio is 8 and its heat of combustion is 30 kJ/g.

(a) Compute the mass burning rate

(b) If the temperature does not change when the hatch is being closed, find the width of the hatch opening (the height stays fixed) enough to just cause the fire to be ventilation-limited.

11.6 A fire burns in a compartment under steady conditions. The fuel supply rate ($\dot{m}_F$) is fixed.
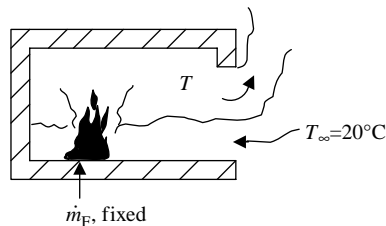

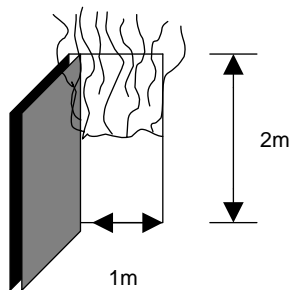Its properties are:

Heat of combustion = 45 kJ/g

Stoichiometric air to fuel mass ratio = 15 g air/g fuel

The ambient temperature is 20 °C and the specific heat of the gases is assumed constant at 1 kJ/kg K. The fuel enters at a temperature of 20 °C. For all burning conditions 40 % of the energy released within the compartment is lost to the walls and exterior by heat transfer.

(a) The compartment has a door 2 m high, which is ajar with a slit 0.01 m wide. The fire is just at the ventilation limit for this vent opening.
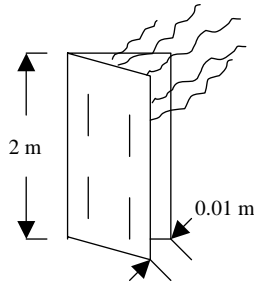
(i) Calculate the exit gas temperature.

(ii) Calculate the airflow rate.

(iii) Calculate the fuel supply rate.

(b) The door is opened to a width of 1 m. Estimate the resulting exit gas temperature. State any assumptions.

11.7 A room in a power plant has a spill of diesel fuel over a 3 m diameter diked area. The compartment is made of 20 cm thick concrete, and the properties are given below. The only opening is a 3 m by 2.5 m high doorway. The dimensions of the compartment are 10 m × 30 m × 5 m high. Only natural convection conditions prevail. The ambient air temperature is 20 °C. Other properties are given below:

Concrete:

$k = 1.0$ W/m K

$\rho = 2000$ kg/m^3

$c = 0.88$ kJ/kg K

Diesel:

Liquid density $= 918$ kg/m^3

Liquid specific heat $= 2.1$ J/g K

Heat of vaporization $= 250$ J/g

Vapor specific heat $= 1.66$ J/g K

Boiling temperature $= 250\,°$C

Stoichiometric air to fuel mass ratio $= 15$

Heat of combustion $= 44.4$ kJ/g

The diesel fuel is ignited and spreads rapidly over the surface, reaching steady burning almost instantly. At this initial condition, compute the following:

(a) The energy release rate.

(b) The flame extent.

(c) The temperature directly above the fuel spill.

(d) The maximum ceiling jet temperature 4 m from the center of the spill.

At 100 s, the burning rate has not significantly changed, and the compartment has reached a quasi-steady condition with countercurrent flow at the doorway. At this new time, compute the following:

(e) The average smoke layer temperature.

(f) The air flow rate through the doorway.

(g) The equivalence ratio, ϕ.

By 400 s, the fuel spill 'feels' the effect of the heated compartment. At this time the fuel surface receives all the heat flux by radiation from the smoke layer, σT^4, over half of its area. For this condition, compute the following:

(h) The energy release rate as a function of the smoke layer temperature, T.

(i) Compute the total rate of losses (heat and enthalpy) as a function of the compartment smoke layer temperature. Assume the heat loss rate per unit area can be estimated by conduction only into the concrete from the gas temperature; i.e. $\sqrt{\frac{k\rho c}{t}}$ is the concrete conductance, where t is taken as 400 seconds.

(j) Plot (h) and (i) to compute the compartment gas temperature. Is the state ventilation-limited?

11.8 Compute the average steady state temperature on a floor due to the following fires in the World Trade Center towers. The building is 63.5 m on a side and a floor is 2.4 m high. The center core is not burning and remains at the ambient temperature of 20 °C. The core dimensions are 24 m × 42 m. For each fuel fire, compute the duration of the fire and the mass flow rate excess fuel or air released from the compartment space. The heat loss from the compartment fire should be based on an overall heat transfer coefficient of 20 W/m^2 K with a sink temperature of 20 °C. The vents are the broken windows and damage openings and these are estimated to be one-quarter of the building perimeter with a height of 2.4 m.

The airflow rate through these vents is given as $0.5A_oH_o^{1/2}$ kg/s with the geometric dimensions in m.

(a) 10 000 gallons of aviation fuel is spilled uniformly over a floor and ignited. Assume the fuel has properties of heptane. Heptane burns at its maximum rate of 70 g/m^2 s.

(b) After the aviation fuel is depleted, the furnishings burn. They can be treated as wood. The wood burns according to the solid curve in Figure 11.17. Assume the shape effect $W_1/W_2 = 1$, A is the floor area and $A_oH_o^{1/2}$ refers to the ventilation factor involving the flow area of the vents where air enters and the height of the vents. The fuel loading is 50 kg/m^2 of floor area.

11.9 Qualitatively sketch the loss rate and gain rate curves for these three fire states: (a) flame just touching the ceiling, (b) the onset of flashover and (c) the stoichiometric state where the fire is just ventilation-limited. Assume the L curve stays fixed in time and is nearly linear.
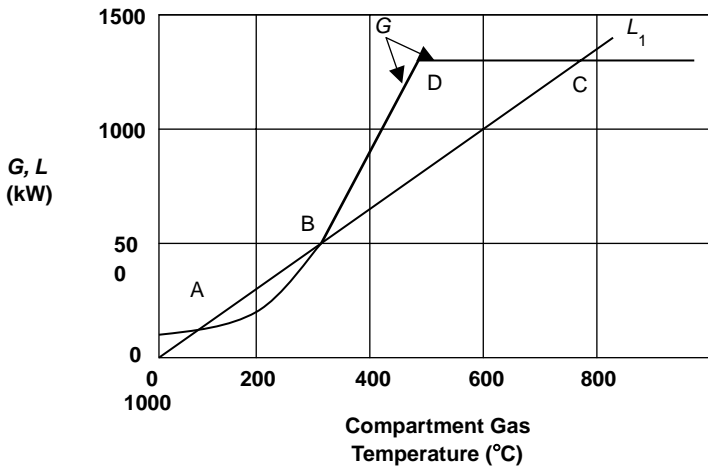
Use the graph above in which the generation rate of energy for the compartment is given by the G curve as a function of the compartment temperature and the loss rate of energy; heat from the compartment is described below.

(a) L_1 represents the loss curve shortly after the fire begins in the compartment. What is the compartment temperature and energy release rate? Identify this point on the above figure.

(b) As the compartment walls heat, the losses decrease and the L curve remains linear. What is the gas temperature just before and after the fire becomes ventilation-limited? Draw the curve and label the points VL− and VL+ respectively.

(c) Firefighters arrive after flashover and add water to the fire, increasing the losses. The loss curve remains linear. What is the gas temperature just before and after the suppression dramatically reduces the fire? Draw this L curve on the above figure. Assume the loss rate to suppression is proportional to the difference between the compartment gas temperature and ambient temperature, $T - T_\infty$.

11.10 Identify the seven elements in the graph with the best statement below:
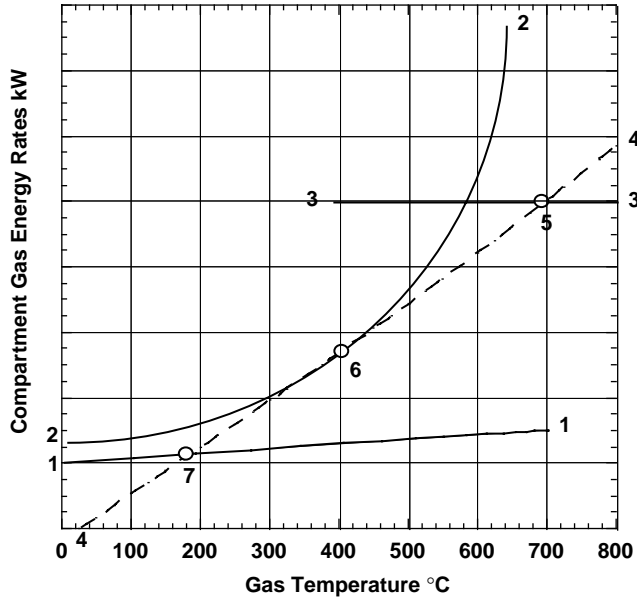
- Heat loss rate _____
- Wood crib firepower _____
- Unstable state _____
- Fully developed fire _____
- Firepower under ventilation-limited conditions _____
- Flashover _____
- Critical state _____
- Stable state _____
- Heat and enthalpy flow rate _____
- Firepower of a burning wall _____